THE JOURNAL OF PHYSICAL CHEMISTRY Letters

Letter

pubs.acs.org/JPCL

Controlling Exciton Diffusion and Fullerene Distribution in Photovoltaic Blends by Side Chain Modification

Muhammad T. Sajjad,[†] Alexander J. Ward,[†] Christian Kästner,[‡,§] Arvydas Ruseckas,[†] Harald Hoppe,[‡,∥,⊥] and Ifor D. W. Samuel*[,†]

[†]Organic Semiconductor Centre, SUPA, School of Physics and Astronomy, University of St. Andrews, St. Andrews, KY16 9SS, United Kingdom

[‡]Institute of Physics, Technische Universität Ilmenau, Langewiesener Straße 22, 98693 Ilmenau, Germany

[§]Institute of Thermodynamics and Fluid Mechanics, Technische Universität Ilmenau, Helmholtzring 1, 98693 Ilmenau, Germany

[∥]Center for Energy and Environmental Chemistry Jena (CEEC Jena), Friedrich Schiller University Jena, Philosphenweg 7a, 07743 Jena, Germany

[⊥]Laboratory of Organic and Macromolecular Chemistry (IOMC), Friedrich Schiller University Jena, Humboldtstrasse 10, 07743 Jena, Germany

Supporting Information

ABSTRACT: The influence of crystallinity on exciton diffusion and fullerene distribution was investigated by blending amorphous and semicrystalline copolymers. We measured exciton diffusion and fluorescence quenching in such blends by dispersing fullerene molecules into them. We find that the diffusion length is more than two times higher in the semicrystalline copolymer than in the amorphous copolymer. We also find that fullerene preferentially mixes into disordered regions of the polymer film. This shows that relatively small differences in molecular structure are important for exciton diffusion and fullerene distribution.

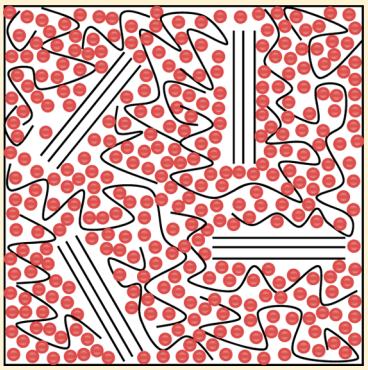

In recent years, organic photovoltaic cells (OPVs) have received significant attention as a promising technology for future power generation due to their attractive properties such as low cost, flexibility, light weight, and ease of fabrication. In these devices, the maximum power conversion efficiencies (7−10%) are achieved by using a heterojunction (BHJ) in which both electron donor and acceptor materials are blended together as the active layer.[1−5] In OPVs, excitons are generated following light absorption and then diffuse to the interface between donor and acceptor, where charge separation occurs. Exciton diffusion is a crucial step because it determines the fraction of excitons that contribute to the extracted photocurrent. The length scale of exciton diffusion determines the device geometry and the desired morphology for high efficiency. Exciton diffusion is also very important for highly efficient organic light emitting devices (OLEDs) and organic lasers because it can lead to either exciton−exciton annihilation or diffusion of excitons to nonradiative quenching sites and hence loss of efficiency.[6,7]

Exciton diffusion has been measured previously in a range of organic semiconductors[8−19] and values of exciton diffusion length ranging from 2 to 2500 nm have been reported[9,11,13−17,20−23,48−50] using a range of different techniques. However, little work has been done to understand how exciton diffusion is influenced by the physical and chemical structure of materials.[12,24,25] Exciton diffusion depends very much on the electronic properties of the film. It proceeds via a series of hops, from one chromophore to another; therefore, the distribution of energies of the chromophores will have a strong influence on the rate of hopping. In a film with a broad spread of energies, an exciton that is created on a high energy site will initially be able to transfer to any of its nearest neighbors, which will likely have lower energies. As time goes on, the exciton will find itself on lower and lower energy sites and have a slower rate of hopping to nearby, usually higher energy sites.[26] This is known as dispersive diffusion and leads to a diffusion coefficient that slows down with time.[26−28] On the other hand, in a film where all the chromophores have approximately the same energy, the exciton can move to any nearest neighbor with approximately the same rate at any time after excitation. The case where the available chromophores are largely isoenergetic will be described well with Fickian diffusion and will have a time independent diffusion coefficient. Typically, this isoenergetic

Received: May 21, 2015
Accepted: July 9, 2015
Published: July 9, 2015

DOI: 10.1021/acs.jpclett.5b01059
J. Phys. Chem. Lett. 2015, 6, 3054−3060

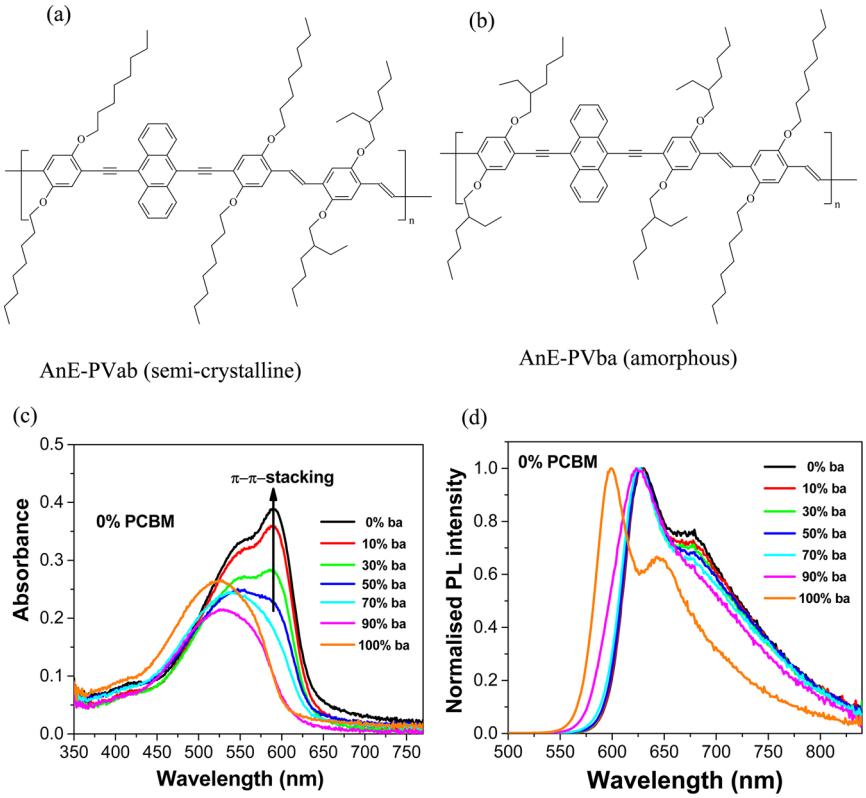

Figure 1. (a) Molecular structure of the semicrystalline (AnE-PVab) polymer. (b) Molecular structure of the amorphous (AnE-PVba). (c) Absorption spectra of the two copolymers and their blends. The graphs are labeled with the percentage of the amorphous copolymer (AnE-PVba) in the sample. (d) Photoluminescence spectra of two AnE-PV copolymers and their blends excited at 400 nm. The graphs are labeled with the percentage of the amorphous copolymer (AnE-PVba) in the sample.

case is favorable for long-range exciton diffusion and is associated with structural order and crystallinity within the film.[12,24,26,29−31]

The degree of crystallinity of the polymer is associated with many other properties of the film including the charge separation efficiency,[32] charge transport,[33,34] and degree of phase segregation between the components.[35−37] As some of these effects are positive and some have a detrimental effect on the device performance, it is often found that materials with intermediate crystallinities give the best power conversion efficiencies.[36,38−40]

An elegant way of exploring the influence of degree of crystallinity on the physical properties is to use a blend of copolymers to vary the degree of order in the film.[33,36,37,41] Here, we investigated two anthracene containing poly(*p*-phenylene-ethynylene)-*alt*-poly(*p*-phenylene-vinylene) (PPE−PPV) copolymers (AnE-PPV) (molecular structures given in Figure 1a and b) that are used as donor materials for solar cell applications.[36,42] The two polymers have the same conjugated backbone but differ in the number and position of branched side chains. The polymer with more branched side chains (AnE-PVba) is amorphous whereas the one with fewer branched side chains (AnE-PVab) is semicrystalline.[36] A reasonably high solar cell efficiency (∼4%) was achieved for ternary blends containing both amorphous (10%) and semicrystalline (90%) material along with PCBM.[36] The ability to modify the overall crystallinity of the film, by changing the blend ratio of amorphous to semicrystalline polymer, makes blends of these polymers an ideal model system to investigate some important unanswered questions in OPV research: How does the crystallinity influence exciton diffusion? what influence does this have on exciton harvesting? How does the polymer's ability to crystallize influence the distribution of acceptor in the blend?

In this Letter, we investigate the influence of polymer crystallinity on exciton diffusion in different blends of photovoltaic materials. We measured the exciton diffusion length in both AnE-PV copolymers and find it to be at least 8.8 nm for the semicrystalline polymer and at least 4.2 nm for the amorphous polymer. We observe that excitons reach the fullerene molecules in the semicrystalline polymer with a time-independent rate constant, whereas there is a pronounced slowing down of this rate constant for the amorphous polymer. This allows us to assign the higher value of exciton diffusion length in semicrystalline material to isoenergetic hopping of excitons (distribution of energy states <0.025 eV) compared to amorphous material in which the exciton transport is dispersive due to a large distribution of hopping energy states on the order of 0.12 eV.

Having established the diffusive behavior of excitons in the pure semicrystalline or amorphous polymers, we were able to characterize how dispersive the quencher was in blends of the semicrystalline polymer and the amorphous polymer. We apply a simple model to determine energy transfer from the amorphous to the semicrystalline polymer in these blends. This allows us to quantify the amount of quenching occurring in amorphous regions and suggests that the PCBM preferentially resides in the amorphous regions, with a concentration 5 times higher than that in the semicrystalline region.

DOI: 10.1021/acs.jpclett.5b01059
J. Phys. Chem. Lett. 2015, 6, 3054−3060

First of all, we measured absorption, photoluminescence (PL) of six samples containing 10, 30, 50, 70, 90, and 100% of amorphous (AnE-PVba) copolymer with the rest of the sample made up of the semicrystalline (AnE-PVab) copolymer. The absorption and photoluminescence spectra of these samples are shown in Figure 1c and d, respectively. The absorption spectrum of the neat amorphous copolymer (100% ba) has a single broad peak around 520 nm. As the content of the semicrystalline polymer increases, an absorption peak at ∼580 nm with a shoulder at 550 nm appears and becomes more pronounced. The 580 nm peak is associated with absorption of the ordered phase of the polymer.[36] The PL spectrum of neat amorphous (100% ba) polymer peaks at 600 nm, whereas spectra of the semicrystalline polymer (0% ba) and binary blends of the two materials peak in the range 625 to 630 nm. The similarity of the spectra of the blends to the spectrum of the semicrystalline polymer shows that emission comes predominantly from the semicrystalline polymer with a strong peak at 630 nm. The strong absorption in the region of 600 nm, and deep red/near-infrared emissions show that there is extensive electron delocalization along the polymer backbone. The fraction of ordered phase (crystallinity fraction) is calculated from the absorption spectra following a procedure reported previously[43] (also given in Supporting Information) and the resulting values are shown in Figure 2. The

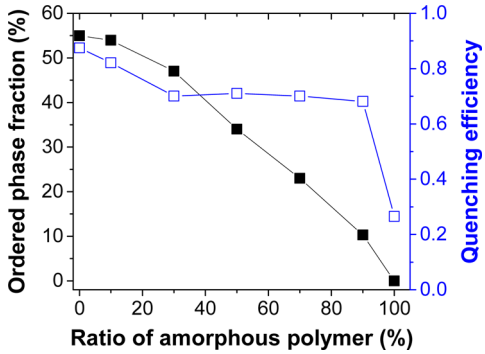

Figure 2. Ordered phase fraction (%) (black dots) calculated using absorption spectra (given in Figure 1c) as a function of different ratios of amorphous polymer (AnE-PVba). Quenching efficiency (1-PLQY ratio) determined by taking the ratio of the PLQY of blends with 1 wt % of PCBM to the PLQY of neat films.

photoluminescence quantum yield (PLQY) of neat samples and samples containing 1 wt % PCBM was measured. This was used to calculate the quenching efficiency by taking the ratio of the PLQY of the sample containing 1 wt % PCBM to the PLQY of neat samples, that is, quenching efficiency = 1 − ((PLQY(with 1 wt % PCBM))/(PLQY(neat sample))). The resulting quenching efficiency is shown in Figure 2 and decreases as the fraction of amorphous polymer increases.

In order to obtain quantitative information about exciton diffusion length and the distribution of energy states, we measured time-resolved fluorescence in blends of neat amorphous and neat semicrystalline polymers with small, known quantities of fullerene (PCBM). Figure 3a shows time-resolved fluorescence as a function of the concentration of fullerene quencher in the amorphous (100% amorphous polymer ba) and semicrystalline (0% amorphous polymer ba) polymers. For a given concentration of quencher the fluorescence decays faster for the semicrystalline polymer

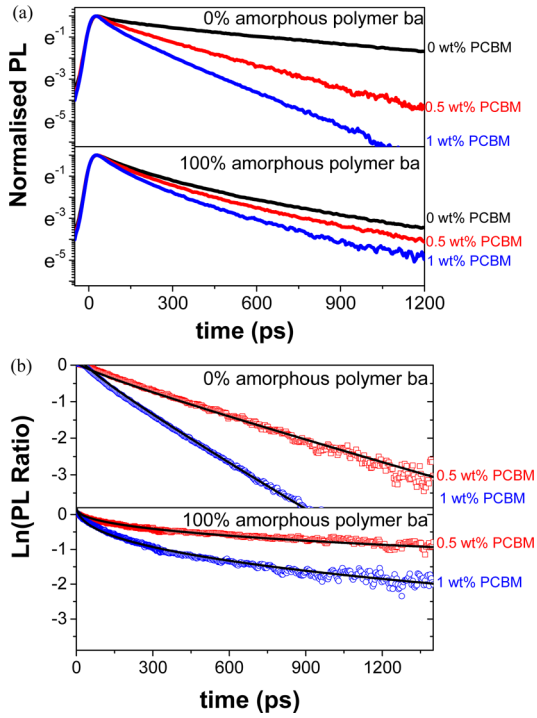

Figure 3. (a) Normalized PL decays of blends of semicrystalline polymer (top) and amorphous (bottom) with low known concentrations of fullerene. (b) Natural logarithm of the ratio of PL of films with low known concentration of quencher to pristine films as a function of time, used to determine diffusion length in the semicrystalline and the amorphous polymer. Black lines are fits to experimental data using eq 4. The obtained value of α from the fits is used to determine the distribution of energy states in the semicrystalline and the amorphous polymers.

than for the amorphous polymer, indicating more quenching is occurring and suggesting a higher exciton diffusion coefficient.

We begin by analyzing the data for films of these two blends, that is, amorphous polymer:PCBM and semicrystalline polymer:PCBM. In order to show additional decay due to quenching caused by the presence of PCBM, we plot the natural logarithms of the ratio of PL decays of films of blends of polymer with 0.5 and 1 wt % of PCBM to PL decay of the pristine film in Figure 3b. It has been shown that the gradients of these lines are equal to the quenching rate of the film.[11] If we approximate the quenching rate as the encounter probability, then we can show

$$\ln[\text{PL ratio}](t) = \int_0^t 4\pi r_q N_q D(t)\mathrm{d}t \tag{1}$$

where r_q is the quenching radius, a distance at which excitons quench instantaneously, $D(t)$ is the time dependent diffusion coefficient and N_q is the total concentration of quenchers. Considering the displacement in a single dimension, the root-mean-square (RMS) displacement of a diffusing species is given by[27]

$$\text{RMS displacement} = \left(2\int_0^t D(t)\mathrm{d}t\right)^{1/2} \tag{2}$$

This 1D RMS displacement is typically known as the diffusion length (L_D) when $t = \tau$, where τ is the lifetime of the neat polymer. Hence the 1D diffusion length can be calculated

DOI: 10.1021/acs.jpclett.5b01059
J. Phys. Chem. Lett. 2015, 6, 3054−3060

directly from the ln (PL ratio), that is, by combining eqs 1 and 2

$$L_D = \left(\frac{\ln[\text{PL ratio}]}{2\pi r_q N_q} \right)^{1/2} \quad (3)$$

The values of r_q = (0.9 ± 0.2) nm and r_q = (0.8 ± 0.2) nm are calculated from spectral overlap between donor and acceptor for amorphous and semicrystalline polymer respectively assuming the quenching mechanism is due to resonance energy transfer from donor to acceptor (details about the calculation are given in Supporting Information). By using these values of r_q, the diffusion lengths of pure amorphous and pure semicrystalline polymers can be determined directly from their corresponding experimental data. A diffusion length of (8.8 ± 0.4) nm was obtained for the semicrystalline polymer and (4.2 ± 0.2) nm for the amorphous polymer. We note that for time independent diffusion this measure of diffusion length would be $\sqrt{(2D\tau)}$ whereas in some publications $\sqrt{(D\tau)}$ has been used.[9,11,15,46,47] This leads to time-averaged diffusion coefficients of (5.9 ± 0.6) × 10^{-4} cm^2/s for semicrystalline and (2.6 ± 0.3) × 10^{-4} cm^2/s for amorphous. The higher value of the diffusion length in the semicrystalline polymer is consistent with previously reported experimental studies of exciton diffusion in organic semiconductors,[12,24] where an enhancement in diffusion coefficient with molecular ordering was observed. However, the enhancement in diffusion length we see is larger. Our results are also consistent with previous studies[28] that correlate exciton diffusion with energetic disorder.

We can learn more about the mechanism of exciton diffusion from the shape of the curves in Figure 3b. The slope of the graph is constant for the semicrystalline polymer but decreasing for the amorphous polymer. This means that the rate constant for quenching is constant for the semicrystalline polymer and decreasing for the amorphous polymer. It leads to a time-independent diffusion coefficient for the semicrystalline polymer and dispersive exciton transport in the amorphous polymer. The latter can be described by a time-dependent diffusion coefficient[27] and as most time-dependent diffusion follows a power law,[26,44] the 100% and 0% amorphous polymer ba experimental data were fitted with

$$\ln(\text{PL ratio}) = -N_q k_0 \frac{t^\alpha}{\alpha} \quad (4)$$

where k_0 is the initial rate of quenching and α is a constant between 0 and 1 that is a measure of the time-dependence of quenching. In addition the time-dependence of the decay gives an indication of the spread of energy levels that the exciton visits during its lifetime. This can be quantified by the following relationship derived from examining the results of Monte Carlo modeling of dispersive diffusion by Schönherr et al.[26]

$$\alpha = \frac{1}{\left(\frac{\sigma}{4kT}\right)^2 + 1} \quad (5a)$$

where σ represents the breadth of the Gaussian distribution of energy states. The resulting values of k_0, α and σ found by fitting the fluorescence decays for blends containing 0% (AnE-PVab) and 100% amorphous (AnE-PVba) polymer (shown in Figure 3) with eqs 4 and 5 are given in Table 1. The fit gives α = 1.00 for the semicrystalline polymer, confirming the time-independent nature of the quenching. The higher value of σ obtained for the case of 100% amorphous (AnE-PVba) polymer indicates a broader energy distribution in the amorphous polymer than the semicrystalline polymer.

Table 1. Initial Rate of Quenching k_0, Dispersive Parameter α, and Breadth of the Gaussian Distribution of Energy States σ Obtained Directly from Experimental Data for the Amorphous and Semicrystalline Material

name	k_0 (nm^3/ps^α)	α	σ
100% amorphous polymer ba	7.3	0.4	5.0 kT
0% amorphous polymer ba	0.6	1.0	≪1kT

As better device efficiency was achieved with a blend containing both amorphous and semicrystalline polymer along with PCBM,[36] we next consider the results for blends containing both the amorphous and semicrystalline polymers and also PCBM. In these blends, we need to consider energy transfer between the two polymers and the distribution of the fullerene between amorphous and semicrystalline phases as well as exciton diffusion. As fluorescence in the mixed blends was coming predominantly from the semicrystalline polymer (Figure 1d), we used time-resolved fluorescence to probe the excitation energy transfer (EET) in mixed blends of amorphous and semicrystalline polymer (in the absence of fullerene acceptor). In order to assign a time constant for the excitation energy transfer, the PL decays from emission on the blue side (between 603 and 611 nm) and the emission from the red side (between 650 and 705 nm) were measured. Both decays (blue and red side) were then normalized at 100 ps and an additional decay, corresponding to energy transfer, was obtained by subtracting the normalized blue side PL decay curve from the equivalent red side PL decay curve. The resulting decays for all blends were fitted at short time to an exponential decay, so that the time constant for the excitation energy transfer for each blend could be measured. This time-resolved EET observed in Figure 4a can be assigned to resonance energy transfer from the amorphous to the crystalline domains. This interpretation is supported by considering that the rate constant for the excitation energy transfer increases with the increasing proportion of semicrystalline polymer (and consequently decreasing proportion of amorphous polymer) in the blend. The rate constants produced ranged from 81 ns^{-1} for the blend with 10% amorphous polymer ba to 16 ns^{-1} for the blend with 90% amorphous polymer ba (see inset of Figure 4a). The rapid rate of transfer in the 10% amorphous blend indicates very efficient exciton transfer from the amorphous phase in this blend and offers an explanation as to why exciton harvesting and device efficiencies remain high in blends even when small amounts of the amorphous polymer are introduced.

We next determine the concentration of quencher in the amorphous and semicrystalline regions. This was done by measuring time-resolved fluorescence in mixed blends of amorphous and semicrystalline polymers with small, known quantities of fullerene (PCBM). The time-resolved fluorescence decays (Supporting Information Figure S3) and ln(PL ratios) (Figure 5) show that quenching is time independent in pure semicrystalline polymer and becomes time dependent as the fraction of amorphous polymer increases. We used the difference in time dependence to predict the distribution of quencher between the amorphous and semicrystalline regions. To do this, we first determined the rate of quenching by fitting the data of neat semicrystalline (0% amorphous polymer ba) polymer at times after 150 ps using eq 4 assuming time-independent quenching (i.e., α = 1). Then by using this

DOI: 10.1021/acs.jpclett.5b01059
J. Phys. Chem. Lett. 2015, 6, 3054−3060

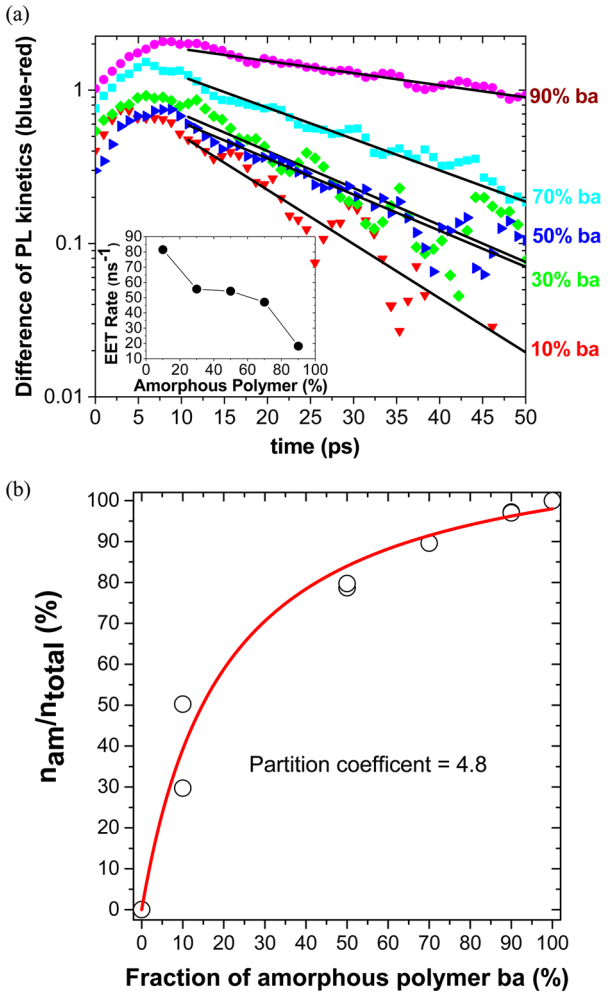

Figure 4. (a) Difference of PL kinetics determined by subtracting emission of blue side (between 603 and 611 nm) and equivalent emission of red side (650−705 nm) as function of time. Excitation energy rate (EET) is determined by fitting an exponential decay to PL kinetics and is given in the inset of Figure 4a as a function of ratio of amorphous polymer (b) ratio of number of quenching sites in the amorphous region (n_{am}) to total quenching sites (n_{total}) in the film as a function of amorphous polymer. A partition coefficient of 4.8 was obtained by fitting data with eq 6.

resulting value for the rate of quenching, the concentration of quencher in the semicrystalline region of all other mixed blends is determined by fitting the experimental data of blends above 150 ps (to make sure that complete EET transfer occurs from amorphous to semicrystalline) with the same time independent eq 4 (i.e., $\alpha = 1$). The fitting results are shown in Figure 5 (black lines) and the resulting value of concentration of quencher in the semicrystalline region is given in Table S2 of the Supporting Information. The concentration of quencher in the amorphous region is calculated using

$$\frac{n_{am} + n_{cryst}}{V_{am} + V_{cryst}} = N_q$$

where n_{am} is the number of quenching sites in the amorphous region and V_{am} is the volume of the amorphous region. Similarly n_{cryst} is the number of quenching sites in the semicrystalline region and V_{cryst} is the volume of the semicrystalline region. Because the fullerene may preferentially enter one or other of the polymers, therefore, the partition

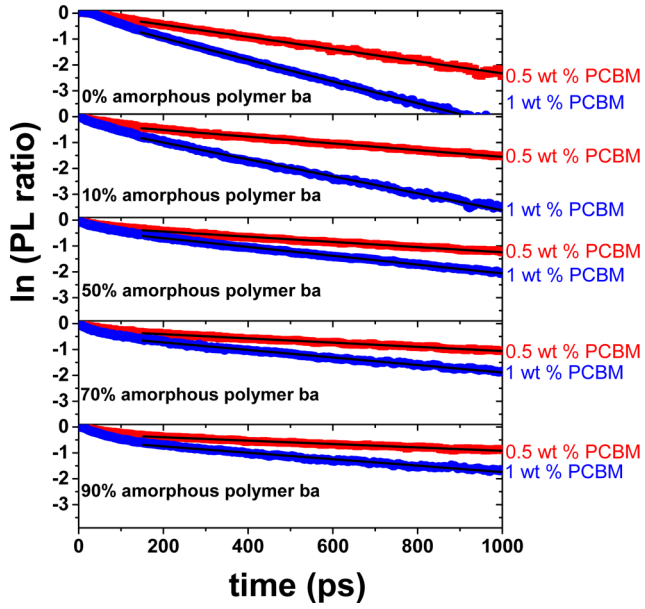

Figure 5. Natural logarithm of the ratio of PL of mixed films with low known concentration of quencher to neat films as a function of time. Black lines are fits to experimental data.

coefficient of the materials, which is the ratio of the equilibrium concentration of PCBM in the amorphous region divided by the equilibrium concentration of PCBM in the semicrystalline polymer, can be determined from the distribution of quencher between amorphous and semicrystalline regions. This is analogous to how a solute will be distributed between two immiscible solvents in contact at equilibrium

$$P_{a/s} = \frac{[\mathrm{PCBM}]_{amorph}}{[\mathrm{PCBM}]_{semicryst}} = \frac{\left(\frac{n_{am}}{V_{am}}\right)}{\left(\frac{n_{cryst}}{V_{cryst}}\right)} \quad (5)$$

This leads to

$$\frac{n_{am}}{n_{total}} = \frac{P_{a/s} r_{am}}{(P_{a/s} r_{am}) + 1} \quad (6)$$

where r_{am} is the ratio of amorphous to semicrystalline polymer in the blend and n_{total} is total number of quenching sites in the blend, that is, $n_{total} = n_{am} + n_{cryst}$.

If we plot (n_{am}/n_{total}) against the actual ratio of amorphous polymer in the blend and fitted with eq 6 (fitting results are shown in Figure 4b), we get a partition coefficient of 4.8, that is, the amount of quencher in the amorphous region is ∼5 times higher than that in the semicrystalline region. This is consistent with other reports which indicated that quencher is expelled from crystalline regions.[36,45]

We also verified our method of finding the concentration of quencher in the amorphous region through an alternative approach. This was done by fitting the data from the blue part of the emission (from 600 to 610 nm) of the 90% amorphous blend below 50 ps (before EET transfer occurs). The obtained value of concentration of quencher is similar to the one determined above. The details are given in Supporting Information.

In conclusion, we have measured the exciton diffusion length in two closely related polymers which differ only in crystallinity and found that the exciton diffusion length in a semicrystalline

DOI: 10.1021/acs.jpclett.5b01059
J. Phys. Chem. Lett. 2015, 6, 3054−3060

polymer is twice as large as in the corresponding amorphous polymer. Furthermore, we found that the semicrystalline polymer exhibits quenching kinetics consistent with isoenergetic hopping and can be described by time-independent diffusion. This could be either because there is less energetic disorder or because the spatial correlations in the energy are on a longer length-scale than the exciton diffusion length. On the other hand, the amorphous polymer has a distribution of energy states on the order of 5 times kT and exciton transport can be described with time-dependent diffusion, that is, dispersive diffusion. A rapid red shift of emission is observed due to resonance energy transfer from the amorphous to the crystalline regions. By investigating mixed blends with different ratios of amorphous and semicrystalline polymer, we found that the concentration of quencher in the amorphous region of the blend is 5 times higher than in the semicrystalline region. Hence, the excitons in the amorphous regions are more likely to encounter electron acceptors due to the superior mixing of the two components in these regions. In addition, resonance energy transfer can efficiently transport remaining excitons out of the amorphous region, despite the relatively slow exciton diffusion. Therefore, this work has wide-ranging implications for rational solar cell design as it demonstrates that though exciton diffusion is faster in crystalline regions, exciton harvesting can be efficient from amorphous regions.

■ ASSOCIATED CONTENT

Supporting Information

The Supporting Information describes the calculation of the fraction of the ordered phase, the quenching efficiency from the PLQY ratio, the Förster radius, the quenching radius and the determination of the number of quenching sites in the amorphous region of the blends. The Supporting Information is available free of charge on the ACS Publications website at DOI: 10.1021/acs.jpclett.5b01059.

■ AUTHOR INFORMATION

Corresponding Author

*E-mail: idws@st-andrews.ac.uk.

Notes

The authors declare no competing financial interest.

■ ACKNOWLEDGMENTS

The authors thank the European Research Council for financial support (grant number 321305). I.D.W.S. acknowledges a Royal Society Wolfson Research Merit Award. A.J.W. is thankful to the Scottish Doctoral Training Centre for financial support (grant number EP/L015110/1) and A.R. is thankful to EPSRC for financial support (grant number EP/J009016). C.K. acknowledges financial support from the "Thüringer Landesgraduiertenschule für Photovoltaik" (PhotoGrad). C.K. and H.H. are grateful to the "Deutsche Forschungsgemeinschaft" (DFG) for financial support within the priority program SPP1355.

■ REFERENCES

(1) Liang, Y.; Xu, Z.; Xia, J.; Tsai, S. T.; Wu, Y.; Li, G.; Ray, C.; Yu, L. For the Bright Future—Bulk Heterojunction Polymer Solar Cells with Power Conversion Efficiency of 7.4%. *Adv. Mater.* **2010**, *22*, E135−E138.

(2) He, Z.; Zhong, C.; Su, S.; Xu, M.; Wu, H.; Cao, Y. Enhanced Power-Conversion Efficiency in Polymer Solar Cells using an Inverted Device Structure. *Nat. Photonics* **2012**, *6*, 591−595.

(3) Zhou, H.; Zhang, Y.; Seifter, J.; Collins, S. D.; Luo, C.; Bazan, G. C.; Nguyen, T. Q.; Heeger, A. J. High-Efficiency Polymer Solar Cells Enhanced by Solvent Treatment. *Adv. Mater.* **2013**, *25*, 1646−1652.

(4) Service, R. Solar energy. Outlook Brightens for Plastic Solar Cells. *Science (Washington, DC, U. S.)* **2011**, *332*, 293.

(5) Green, M. A.; Emery, K.; Hishikawa, Y.; Warta, W.; Dunlop, E. D. Solar Cell Efficiency Tables (version 44). *Prog. Photovoltaics* **2014**, *22*, 701−710.

(6) Samuel, I. D. W.; Rumbles, G.; Collison, C. J.; Friend, R. H.; Moratti, S. C.; Holmes, A. B. Picosecond Time-Resolved Photoluminescence of PPV Derivatives. *Synth. Met.* **1997**, *84*, 497−500.

(7) Antoniadis, H.; Rothberg, L. J.; Papadimitrakopoulos, F.; Yan, M.; Galvin, M. E.; Abkowitz, M. A. Enhanced Carrier Photogeneration by Defects in Conjugated Polymers and its Mechanism. *Phys. Rev. B: Condens. Matter Mater. Phys.* **1994**, *50*, 14911.

(8) Lewis, A. J.; Ruseckas, A.; Gaudin, O. P. M.; Webster, G. R.; Burn, P. L.; Samuel, I. D. W. Singlet Exciton Diffusion in MEH-PPV Films Studied by Exciton−Exciton Annihilation. *Org. Electron.* **2006**, *7*, 452−456.

(9) Shaw, P. E.; Ruseckas, A.; Samuel, I. D. W. Exciton Diffusion Measurements in Poly (3-hexylthiophene). *Adv. Mater.* **2008**, *20*, 3516−3520.

(10) Shaw, P. E.; Ruseckas, A.; Peet, J.; Bazan, G. C.; Samuel, I. D. W. Exciton−Exciton Annihilation in Mixed-Phase Polyfluorene Films. *Adv. Funct. Mater.* **2010**, *20*, 155−161.

(11) Ward, A. J.; Ruseckas, A.; Samuel, I. D. W. A Shift from Diffusion Assisted to Energy Transfer Controlled Fluorescence Quenching in Polymer−Fullerene Photovoltaic Blends. *J. Phys. Chem. C* **2012**, *116*, 23931−23937.

(12) Masri, Z.; Ruseckas, A.; Emelianova, E. V.; Wang, L.; Bansal, A. K.; Matheson, A.; Lemke, H. T.; Nielsen, M. M.; Nguyen, H. A.; Coulembier, O.; et al. Molecular Weight Dependence of Exciton Diffusion in Poly (3-hexylthiophene). *Adv. Energy Mater.* **2013**, *3*, 1445−1453.

(13) Bruno, A.; Reynolds, L. X.; Dyer-Smith, C.; Nelson, J.; Haque, S. A. Determining the Exciton Diffusion Length in a Polyfluorene from Ultrafast Fluorescence Measurements of Polymer/Fullerene Blend Films. *J. Phys. Chem. C* **2013**, *117*, 19832−19838.

(14) Raisys, S.; Kazlauskas, K.; Daskeviciene, M.; Malinauskas, T.; Getautis, V.; Jursenas, S. Exciton Diffusion Enhancement in Triphenylamines via Incorporation of Phenylethenyl Sidearms. *J. Mater. Chem. C* **2014**, *2*, 4792−4798.

(15) Menke, S. M.; Luhman, W. A.; Holmes, R. J. Tailored Exciton Diffusion in Organic Photovoltaic Cells for Enhanced Power Conversion Efficiency. *Nat. Mater.* **2012**, *12*, 152−157.

(16) Markov, D. E.; Amsterdam, E.; Blom, P. W. M.; Sieval, A. B.; Hummelen, J. C. Accurate Measurement of the Exciton Diffusion Length in a Conjugated Polymer using a Heterostructure with a Side-Chain Cross-Linked Fullerene Layer. *J. Phys. Chem. A* **2005**, *109*, 5266−5274.

(17) Scully, S. R.; McGehee, M. D. Effects of Optical Interference and Energy Transfer on Exciton Diffusion Length Measurements in Organic Semiconductors. *J. Appl. Phys.* **2006**, *100*, 034907.

(18) Markov, D. E.; Blom, P. W. M. Anisotropy of Exciton Migration in Poly (p-phenylene vinylene). *Phys. Rev. B: Condens. Matter Mater. Phys.* **2006**, *74*, 085206.

(19) Kroeze, J. E.; Savenije, T. J.; Vermeulen, M. J. W.; Warman, J. M. Contactless Determination of the Photoconductivity Action Spectrum, Exciton Diffusion Length, and Charge Separation Efficiency in Polythiophene-Sensitized TiO2 Bilayers. *J. Phys. Chem. B* **2003**, *107*, 7696−7705.

(20) Heremans, P.; Cheyns, D.; Rand, B. P. Strategies for Increasing the efficiency of Heterojunction Organic Solar Cells: Material Selection and Device Architecture. *Acc. Chem. Res.* **2009**, *42*, 1740−1747.

(21) Mikhnenko, O. V.; Cordella, F.; Sieval, A. B.; Hummelen, J. C.; Blom, P. W. M.; Loi, M. A. Temperature Dependence of Exciton Diffusion in Conjugated Polymers. *J. Phys. Chem. B* **2008**, *112*, 11601−11604.

DOI: 10.1021/acs.jpclett.5b01059
J. Phys. Chem. Lett. 2015, 6, 3054−3060

(22) Gregg, B. A.; Sprague, J.; Peterson, M. W. Long-Range Singlet Energy Transfer in Perylene Bis (phenethylimide) Films. *J. Phys. Chem. B* **1997**, *101*, 5362−5369.
(23) Theander, M.; Yartsev, A.; Zigmantas, D.; Sundström, V.; Mammo, W.; Andersson, M.; Inganäs, O. Photoluminescence Quenching at a Polythiophene/C 60 Heterojunction. *Phys. Rev. B: Condens. Matter Mater. Phys.* **2000**, *61*, 12957.
(24) Lin, J. D. A.; Mikhnenko, O. V.; Chen, J.; Masri, Z.; Ruseckas, A.; Mikhailovsky, A.; Raab, R. P.; Liu, J.; Blom, P. W. M.; Loi, M. A.; et al. Systematic Study of Exciton Diffusion Length in Organic Semiconductors by Six Experimental Methods. *Mater. Horiz.* **2014**, *1*, 280−285.
(25) Li, Z.; Zhang, X.; Woellner, C. F.; Lu, G. Understanding Molecular Structure Dependence of Exciton Diffusion in Conjugated Small Molecules. *Appl. Phys. Lett.* **2014**, *104*, 143303.
(26) Schnönherr, G.; Eiermann, R.; Bässler, H.; Silver, M. Dispersive Exciton Transport in a Hopping System with Gaussian Energy Distribution. *Chem. Phys.* **1980**, *52*, 287−298.
(27) Burlakov, V. M.; Kawata, K.; Assender, H. E.; Briggs, G. A. D.; Ruseckas, A.; Samuel, I. D. W. Discrete Hopping Model of Exciton Transport in Disordered Media. *Phys. Rev. B: Condens. Matter Mater. Phys.* **2005**, *72*, 075206.
(28) Athanasopoulos, S.; Emelianova, E. V.; Walker, A. B.; Beljonne, D. Exciton Diffusion in Energetically Disordered Organic Materials. *Phys. Rev. B: Condens. Matter Mater. Phys.* **2009**, *80*, 195209.
(29) Najafov, H.; Lee, B.; Zhou, Q.; Feldman, L.; Podzorov, V. Observation of Long-Range Exciton Diffusion in Highly Ordered Organic Semiconductors. *Nat. Mater.* **2010**, *9*, 938−943.
(30) Yoo, S.; Domercq, B.; Kippelen, B. Efficient Thin-Film Organic Solar Cells Based on Pentacene/C 60 Heterojunctions. *Appl. Phys. Lett.* **2004**, *85*, 5427−5429.
(31) Huijser, A.; Savenije, T. J.; Meskers, S. C.; Vermeulen, M. J.; Siebbeles, L. D. The Mechanism of Long-Range Exciton Diffusion in a Nematically Organized Porphyrin Layer. *J. Am. Chem. Soc.* **2008**, *130*, 12496−12500.
(32) Ohkita, H.; Cook, S.; Astuti, Y.; Duffy, W.; Tierney, S.; Zhang, W.; Heeney, M.; McCulloch, I.; Nelson, J.; Bradley, D. D. C. Charge Carrier Formation in Polythiophene/Fullerene Blend Films Studied by Transient Absorption Spectroscopy. *J. Am. Chem. Soc.* **2008**, *130*, 3030−3042.
(33) Jiang, X. M.; Osterbacka, R.; Korovyanko, O.; An, C. P.; Horovitz, B.; Janssen, R. A.; Vardeny, Z. V. Spectroscopic Studies of Photoexcitations in Regioregular and Regiorandom Polythiophene Films. *Adv. Funct. Mater.* **2002**, *12*, 587−597.
(34) Herrmann, D.; Niesar, S.; Scharsich, C.; Köhler, A.; Stutzmann, M.; Riedle, E. Role of Structural Order and Excess Energy on Ultrafast Free Charge Generation in Hybrid Polythiophene/Si Photovoltaics Probed in Real Time by Near-Infrared Broadband Transient Absorption. *J. Am. Chem. Soc.* **2011**, *133*, 18220−18233.
(35) Campoy-Quiles, M.; Kanai, Y.; El-Basaty, A.; Sakai, H.; Murata, H. Ternary mixing: A Simple Method to Tailor the Morphology of Organic Solar Cells. *Org. Electron.* **2009**, *10*, 1120−1132.
(36) Kästner, C.; Rathgeber, S.; Egbe, D. A. M.; Hoppe, H. Improvement of Photovoltaic Performance by Ternary Blending of Amorphous and Semi-crystalline Polymer Analogues with PCBM. *J. Mater. Chem. A* **2013**, *1*, 3961−3969.
(37) Jamieson, F. C.; Domingo, E. B.; McCarthy-Ward, T.; Heeney, M.; Stingelin, N.; Durrant, J. R. Fullerene Crystallisation as a Key Driver of Charge Separation in Polymer/Fullerene Bulk Heterojunction Solar Cells. *Chem. Science* **2012**, *3*, 485−492.
(38) Moulé, A. J.; Meerholz, K. Controlling Morphology in Polymer−Fullerene Mixtures. *Adv. Mater.* **2008**, *20*, 240−245.
(39) Berson, S.; De Bettignies, R.; Bailly, S.; Guillerez, S. Poly (3-hexylthiophene) Fibers for Photovoltaic Applications. *Adv. Funct. Mater.* **2007**, *17*, 1377−1384.
(40) Khlyabich, P. P.; Burkhart, B.; Thompson, B. C. Compositional Dependence of the Open-Circuit Voltage in Ternary Blend Bulk Heterojunction Solar Cells Based on Two Donor Polymers. *J. Am. Chem. Soc.* **2012**, *134*, 9074−9077.
(41) Mangold, H.; Bakulin, A. A.; Howard, I. A.; Kästner, C.; Egbe, D. A. M.; Hoppe, H.; Laquai, F. Control of Charge Generation and Recombination in Ternary Polymer/Polymer: Fullerene Photovoltaic Blends using Amorphous and Semi-Crystalline Copolymers as Donors. *Phys. Chem. Chem. Phys.* **2014**, *16*, 20329−20337.
(42) Egbe, D. A. M.; Turk, S.; Rathgeber, S.; Kuhnlenz, F.; Jadhav, R.; Wild, A.; Birckner, E.; Adam, G.; Pivrikas, A.; Cimrova, V.; et al. Anthracene Based Conjugated Polymers: Correlation Between $\pi-\pi$-Stacking Ability, Photophysical Properties, Charge Carrier Mobility, and Photovoltaic Performance. *Macromolecules* **2010**, *43*, 1261−1269.
(43) Steyrleuthner, R.; Schubert, M.; Howard, I.; Klaumünzer, B.; Schilling, K.; Chen, Z.; Saalfrank, P.; Laquai, F. d. r.; Facchetti, A.; Neher, D. Aggregation in a High-Mobility N-Type Low-Bandgap Copolymer with Implications on Semicrystalline Morphology. *J. Am. Chem. Soc.* **2012**, *134*, 18303−18317.
(44) Ben-Avraham, D.; Havlin, S. *Diffusion and Reactions in Fractals and Disordered systems*; Cambridge University Press: Cambridge, U.K., 2000; Vol. *1*.
(45) Collins, B. A.; Gann, E.; Guignard, L.; He, X.; McNeill, C. R.; Ade, H. Molecular Miscibility of Polymer− Fullerene Blends. *J. Phys. Chem. Lett.* **2010**, *1*, 3160−3166.
(46) Menke, S. M.; Holmes, R. J. Exciton Diffusion in Organic Photovoltaic Cells. *Energy Environ. Sci.* **2014**, *7*, 499−512.
(47) Lin, J. D.; Mikhnenko, O. V.; van der Poll, T. S.; Bazan, G. C.; Nguyen, T. Q. Temperature Dependence of Exciton Diffusion in a Small-Molecule Organic Semiconductor Processed With and Without Additive. *Adv. Mater.* **2015**, *27*, 2528−2532.
(48) Mikhnenko, O. V.; Azimi, H.; Scharber, M.; Morana, M.; Blom, P. W. M.; Loi, M. A. Exciton Diffusion Length in Narrow Bandgap Polymers. *Energy Environ. Sci.* **2012**, *5*, 6960−6965.
(49) Mikhnenko, O. V.; Lin, J.; Shu, Y.; Anthony, J. E.; Blom, P. W. M.; Nguyen, T.-Q.; Loi, M. A. Effect of Thermal Annealing on Exciton Diffusion in a Diketopyrrolopyrrole Derivative. *Phys. Chem. Chem. Phys.* **2012**, *14*, 14196−14201.
(50) Pinto, R. M.; Macoas, E. M. S.; Neves, A. I.; Raja, S.; Baleizão, C. M.; Santos, I. C.; Alves, H. Effect of Molecular Stacking on Exciton Diffusion in Crystalline Organic Semiconductors. *J. Am. Chem. Soc.* **2015**, *137*, 7104−7110.

DOI: 10.1021/acs.jpclett.5b01059
J. Phys. Chem. Lett. 2015, 6, 3054−3060